Proceedings of the ASME 2019 International Design Engineering Technical Conferences & Computers and Information in Engineering Conference
IDETC/CIE 2019
August 18-21, 2019, Anaheim, California, USA

DETC2019/MESA-12345

DEVELOPMENT AND EXPERIMENTAL EVALUATION OF A QUAD-TILT-WING FLYING ROBOT PLATFORM

A. Aihaitijiang
WPI Soft Robotics Lab
Robotics Engineering Program
Worcester Polytechnic Institute
100 Institute Rd, Worcester, MA 01609
E-mail: aaihaitijiang@wpi.edu

Cagdas D. Onal*
Mechanical Engineering Department
Robotics Engineering Program
Worcester Polytechnic Institute
100 Institute Rd, Worcester, MA 01609
E-mail: cdonal@wpi.edu

ABSTRACT

In this paper, we present the mechanical design and control system of a new indoor and outdoor Quad-Tilt-Wing flying robot. The proposed flying robot can achieve vertical takeoff, hovering, and long duration horizontal high-speed flight. All of these flight modes can be achieved by simply changing the angle of the rotors and wings by a tilt mechanism. We present the details on design and prototyping, the attitude control system, and experimental results, including wind-tunnel experiments, full flight tests, and performance tests. The experimental results show that our Quad-Tilt-Wing flying robot successfully achieves full conversion flight: vertical and rapid takeoff, high-speed cruise, and vertical landing. Performance test results show that during horizontal flight, the wings generate lift and effectively reduce energy use compared to a fixed quad rotor architecture. Consequently, the proposed platform combines unique features of multi-rotor and fixed wing systems to achieve long-duration flight with low-energy compared to a conventional multi-rotor UAV.

1 Introduction

Unmanned aerial vehicles (UAVs) are used to accomplish tasks that are dangerous, impractical, or unnecessarily expensive to be performed by an on-board human pilot. A UAV (or flying robot) can enter environments that are dangerous to human life. Fixed wing UAVs have the advantage of being able to fly at high speeds for long durations with a relatively simple structure.

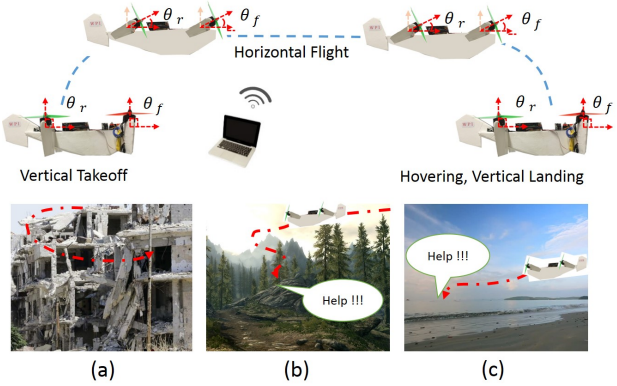

FIGURE 1. Concept Full Conversion Flight of Quad-Tilt-Wing UAV and Concept Illustrations: (a) Indoor Rescue Efforts. (b) Outdoor Search and Rescue. (c) Deliver Life Preservers on High Seas.

Small-scale and fixed-wing aerial vehicles are getting more attention from robotics researchers due to their usability in highly cluttered environments [1–3]. On the other hand, However, fixed-wing flying robots require runways or additional launch and recovery equipment for takeoff and landing [4]. Rotary wing UAVs are able to hover, takeoff, and land vertically with agile maneuvering capability even at very low speeds [5–7]. The hovering and vertical takeoff and landing (VTOL) ability is gained at the expense of high mechanical complexity, high energy use,

*Address all correspondence to this author.

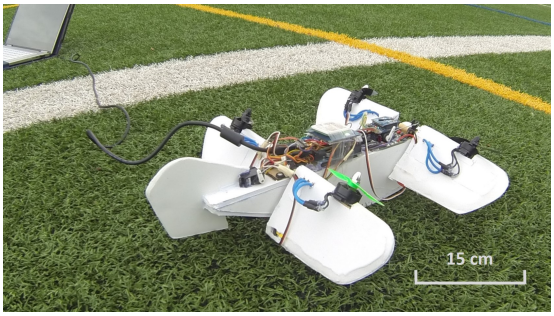

FIGURE 2. Quad-Tilt-Wing UAV Prototype.

low speed, and consequently short flight range [8]. Recently, a new kind of aerial vehicle has appeared, called 'convertible aircraft', which combines the advantages of the rotary-wing and fixed-wing aircrafts. Tilt-rotor UAVs constitute an attractive research area due to their stability and controllability [9–11]. A famous tilt-rotor type UAV is the "Eagle Eye" manufactured by Bell Helicopter [12]. This system has two rotors with a tilt mechanism on the tip of its wing. It can realize vertical takeoff and landing, hovering, and high-cruise-speed flight by changing the angle of the rotors by a tilt mechanism. The disadvantage of using one or two rotors is that it is impossible to fly when one rotor has a malfunction [13, 14]. Additionally, this architecture needs a complex rotor pitch mechanism. Hence, we conclude that for tilt-rotor type UAVs, it is desirable to have four rotors. Such an architecture can continue to fly when one rotor fails, despite at a lower performance, using the remaining three rotors. There are studies on quad-tilt-wing UAVs [15–17]. In the field of tilt wing aircraft, [18] investigated the aerodynamic characteristics of tilt-wing UAV by performing a series of wind tunnel tests. Similar to our proposed system, these existing quad-tilt-wing platforms have four rotors and wings and a tilt mechanism for each rotor. Additionally, they utilize flaperons for each wing. They achieve stability in the rolling direction using the difference of the lift force between flaperons. This mechanical design leads to control system complexity, since two different flight controllers are used for hovering and horizontal flight.

In this paper, we present a new flying robot that combines the advantages of fixed wing and rotary wing UAVs, by using rotor thrust as a source of lift in vertical flight, operating rotors as the forward propulsion sources, and wings as the lift sources in horizontal flight (Fig. 1). We characterized lift and drag coefficients of the wing and measured our flying robot platform's energy efficiency. Unlike current and previous twin-engine tilt wing vehicles and Quad-Tilt-Wing rotor vehicles, our Quad-Tilt-Wing platform does not require additional flaperon, elevator, or rudder control surfaces, which simplifies the control and has advantages over existing systems in payload carrying performance and energy efficiency. We describe the mechanical design, prototyping principles and force analysis of our flying robot platform, the attitude and altitude control system, and the experimental results of our wind tunnel test and full-conversion flight. Performance test results of the flying robot platform on linear and circular paths show that, during horizontal flight, wings contribute to lift and effectively reduce energy expenditure compared to pure vertical quad-rotor flight.

TABLE 1. Specification and Parameters of the UAV

Design Specification	Value	Unit
Fuselage Length	0.38	m
Arm Length (L)	0.15	m
Propeller Length	0.127	m
Propeller Width	0.014	m
Wing Length (Each)	0.15	m
Wing Width (Each)	0.09	m
Each Wing Area($\times$ 4)	0.012	m^2
Total Weight(include battery)	7.22	N
Motor Thrust (Each Motor)	3.33	N
Available Speed	0 - 17	m/s

2 Design and Prototyping

In this section, we describe the physical components of the Quad-Tilt-Wing UAV constructed. The platform was designed to take off and land vertically, hover, fly horizontally, and aimed to be compact for indoor and outdoor use. The design is specifically considered to minimize cost, and offer simple and versatile implementation. The basic concept and prototype of the Quad-Tilt-Wing UAV are presented in Fig. 1 and Fig. 2. The Quad-Tilt-Wing UAV has a tandem wing configuration. Brushless DC motors and propellers are installed on each of the front and rear wing pairs. We can achieve horizontal flight by changing the angle of the rotors and wings using tilt mechanisms made of simple four-bar linkages. Additionally, the front and rear wings have independent tilt mechanisms. The design specifications of the vehicle are tabulated in Table 1.

2.1 Mechanical and Aerodynamic Design Details

The CAD model prepared for the construction and complete assembly of the Quad-Tilt-Wing UAV is shown in Fig. 3. The shape of the wing is a symmetric platform, which ensures no off-center forces during vertical flight, while generating lift in horizontal flight with a finite angle-of-attack. This saves energy following flat-plate aerodynamics. The motors are mounted on the leading edge of the wings to make this small Quad-Tilt-Wing UAV lightweight and strong. We consider this prototype model as a platform for research, and its simplicity makes replication

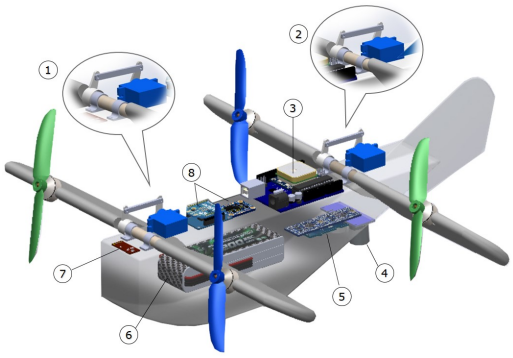

FIGURE 3. CAD Model of the Quad-Tilt-Wing UAV:(1) Front Tilt Mechanism (2) Rear Tilt Mechanism (3) Main Control Board and GPS Module (4) Ultrasonic Sensor (5) Tracking System (6) Battery (7) Current Sensor (8) IMU and XBee module

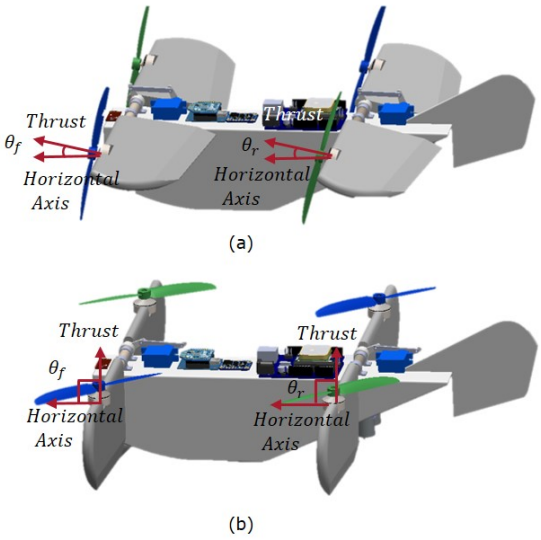

FIGURE 4. Tilt Mechanism of Quad-Tilt-Wing UAV: (a) Horizontal Flight(θ_f and $\theta_r < 90$) (b) Vertical Take off(θ_f and $\theta_r = 90$)

and maintenance easier. The fuselage front view is designed as a rectangle, considering the wing size and embedded electrical components. The fuselage height is the same as wing cord length, which makes the robot have same height when the tilt angle is 90 degrees (vertical flight). One advantage of this design is to ensure that the wings do not contact the ground during take off and landing. Another advantage is that we can use the large space inside the fuselage to place the battery, sensors, micro controller, and other subsystems, to help decrease drag forces. The shape of the wing is selected to be a symmetric flat plate. We assume a flat-plate wing configuration for lift and drag forces, considering the airflow over a flat plate.

The center of mass is located in the middle of the front and rear wings. Because the forces on the rear wings are affected by the airflow around the front wings, if the front and rear wings have the same tilt angle the Quad-Tilt-Wing platform can not achieve passive pitch balance during horizontal flight. We considered two solutions to this issue.We can use an active control system when the fuselage is desired to be kept horizontal (or at any other desired static pitch angle). If the front and rear wings tilt at same angle, we can control the amount of thrust for the front and rear rotors to keep the whole body in balance. In other words, the rear rotors should apply a higher thrust than the front rotors for improved pitch stability. We assume that the tilt angle remains above 25 degrees because the flat plate construction for the wings requires a positive attack angle to generate lift. In this paper, we implemented a controller for the thrust values for pitch stability. We also ensured that the tilt mechanisms for the front and rear wings tilt independently, giving us another control input to the system which may be useful for aggressive maneuvers we may target in future research.

2.2 Tilt Mechanism, Forces and Torques

We achieved horizontal flight using simple four-bar linkage tilt mechanisms, which were used to control the tilt angle of the wings and rotors moving together (Fig. 3 and 4). Servo motors drive the front and rear tilt mechanisms. As a standard, we calibrated the no-tilt condition to 90 degrees (i.e. vertical rotors). Thus, when the tilt angle is at zero degrees, the wings are horizontal and parallel to the fuselage. When the tilt angle is 90 degrees, the wings are vertical and perpendicular to the fuselage long axis. Since rotors are mounted on the wing, the thrust vectors change with the tilt angle [19]. In vertical flight, the thrust forces are all vertical and supply lift, so the Quad-Tilt-Wing UAV can hover and perform VTOL functions. In horizontal flight, the rotor's thrust will contribute to lift and propulsion as a simple function of tilt angle, which will let the Quad-Tilt-Wing UAV move forward (or backward, although this feature is not implemented within the scope of this paper).

Rotors' Generated Forces: We can assume that the thrust force is produced by the i^{th} propeller pushing air. It can be modeled as $F_i = k\omega_i^2$, where k is the thrust coefficient and ω_i^2 denotes the angular speed of each motor. When the rotor tilts at an angle θ_f and θ_r, then the generated force can be resolved into its components along the x and z axes(Fig. 5a). It follows that the i^{th} rotor generated force is:

$$F_i = \begin{pmatrix} k\omega_i^2 \sin(\theta_{f,r}) \\ 0 \\ k\omega_i^2 \cos(\theta_{f,r}) \end{pmatrix} \tag{1}$$

The total generated force due to the four spinning propellers is:

$$F = \sum_{i=1}^{4} F_i = \sum_{i=1}^{4} k\omega_i^2 \tag{2}$$

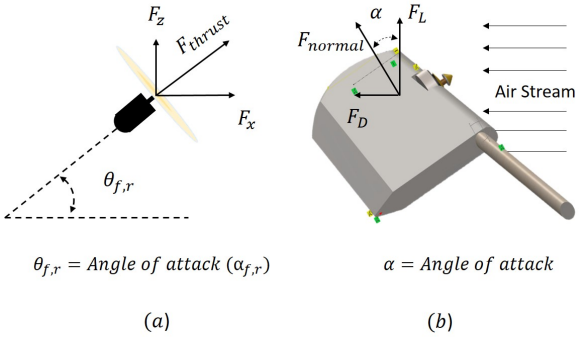

FIGURE 5. Forces: (a) Generated by Rotor (b) Generated by Wing

Gravitational force F_G and drag force F_D are: $F_G = [0,0,-mg]^T$ and drag force defined as $F_{Drag} = -K_d\dot{P} = [-k_d\dot{x},-k_d\dot{y},-k_d\dot{z}]^T$. The total force acting on the quadcopter body is the vector sum of the above three individual forces.

Wings' Generated Forces: As shown in Fig. 5b, the angles of attack (α) and $\theta_{f,r}$ are the same. A fluid flowing over a wing generates lift and drag forces. Lift is the component of this force that is perpendicular to the oncoming flow direction. The drag force which is the component parallel to the flow direction. The Lift and Drag forces are defined as:

$$F_{L_{(Wing)}} = C_L\frac{1}{2}\rho AU^2, \quad F_{D_{(Wing)}} = C_D\frac{1}{2}\rho AU^2 \tag{3}$$

Where, F_L is lift force, and F_D is the drag force. C_L and C_D are lift and drag coefficients. ρ is the mass density of the fluid, U is the flow speed, and A, is the reference area. We can define total forces as a combination of the rotors' generated forces and wings' generated forces. In section 3.1, the lift and drag coefficients are defined through a wind tunnel experiment.

Torque: It is a result of the four rotor's generated forces around the center of gravity. The total moment due to the rotors' generated forces is:

$$M_T = \sum_{i=1}^{4}(L_i \times F_i) \tag{4}$$

Where L_i is a vector directed from the CoG to the i_{th} rotor (Fig. 6), F_i is defined from Eq. 1. Aerodynamic drag torque is the counter rotating torque due to air drag caused by the propeller spinning. When the rotors are tilted with angle α, then the drag torques of the i_{th} propeller are resolved into x and z components as:

$$M_{D,i} = \begin{pmatrix} (-1)^i b\omega_i^2 \sin(\theta_{f,r}) \\ 0 \\ (-1)^i b\omega_i^2 \cos(\theta_{f,r}) \end{pmatrix} \tag{5}$$

Where b is the rotor drag coefficient and the factor $(-1)^i$ is negative for the propellers rotating clockwise (CW). The total torque

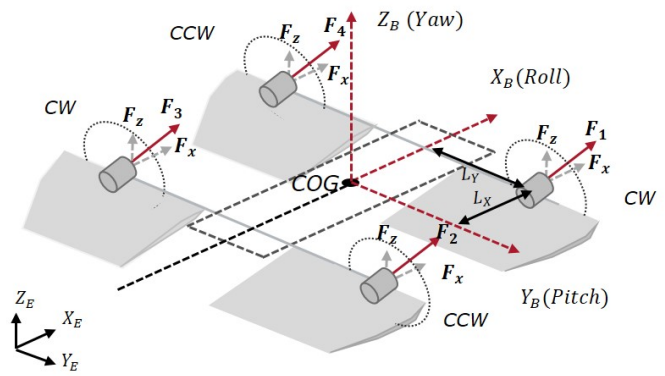

FIGURE 6. Model of Quad-Tilt-Wing Flying Robot

acting on the Quad-Tilt-Wing body is the vector sum of the above two individual torques: $M_{total} = M_T + M_{D,i}$. The Quad-Tilt-Wing dynamic and the equations of motion can be expressed using the typical Newton-Euler formalization [20].

2.3 Control Principles

As shown in Fig. 3 the Quad-Tilt-Wing UAV design is based on an H-shaped quad-rotor structure in vertical flight [21]. Therefore, the center of mass is located between the front and rear wings. We utilize motor thrusts and independent front and rear wing incidence angles for the control of Quad-Tilt-Wing UAV. As in traditional quad-rotors, in vertical flight mode, the roll moment is generated by the difference between the left and right rotor speeds, and the pitch moment is generated by the difference between the front and rear rotor speeds. As shown in Fig. 6, two of the rotors rotate clockwise and two rotate counter-clockwise (in diagonal pairs). The yaw moment is generated by the difference between diagonal rotor speeds [21, 22]. During horizontal flight, the rotors tilt with angle α, so the generated force can be resolved into its components along x and z axes. Similarly, the drag torque of the i^{th} propeller is resolved into x and z components (Eq. 5). The tilt angle α is used to control the forward speed of the Quad-Tilt-Wing flying robot. The front and rear tilt mechanisms are driven by servo motors. We use the same orientation controller for both vertical and horizontal flight. PID controllers keep the flying robot platform's attitude to the required roll (ϕ_d), pitch (θ_d) and yaw (ψ_d) angles. The inputs to our Quad-Tilt-Wing system consist of the angular velocities of each rotor $\gamma_i = \omega_i^2$. We can then solve for each unknown input $[\gamma_1,\gamma_2,\gamma_3,\gamma_4]^T$. The PID controller stabilizes the Quad-Tilt-Wing. The altitude error signal is formed by subtracting the measured altitude (z position) from desired elevation z_d, then using the PID controller to achieve the required altitude 1m. The controller then adjusts the value of control inputs $[\gamma_1,\gamma_2,\gamma_3,\gamma_4]^T$. In the experimental flight tests, each different tilt angle required different altitude control parameters.

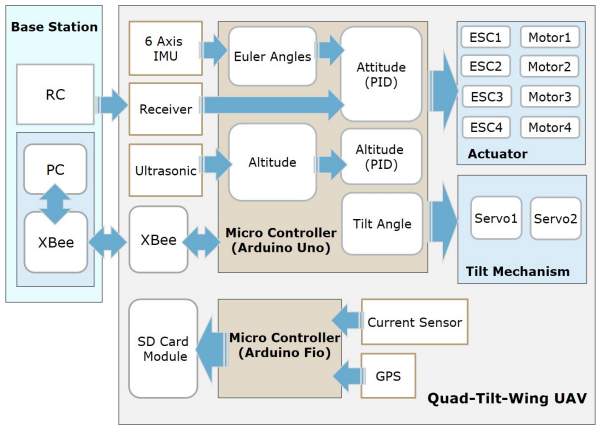

FIGURE 7. System Architecture of Quad-Tilt-Wing UAV

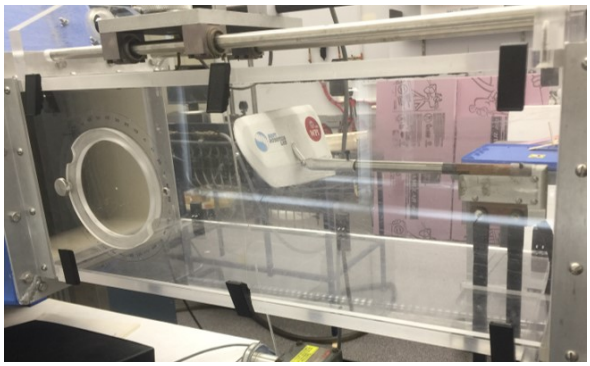

FIGURE 8. Wind Tunnel Test

2.4 Hardware Components

Brushless Motor: The motors we specifically use are Emax MT2204 2300KV (4) brushless DC motors. We chose these motors as they provide a good combination of large thrust and low weight. Each motor weighs 25 g and is rated to 20 A at 12 V. We tested the thrust using LJI 5030 propellers (2 clockwise and 2 counter-clockwise). The maximum thrust was 340 g for each motor.

Electronic Speed Controller: The electronic speed controller converts the available battery voltage to a 3-phase commutation and also regulates the speed of the brushless motors by taking a PWM signal from the control board. In this study we used 20A ESC for each motor.

Control Board: The control board is the main on-board control system which is connected to the sensors, receiver, and electronic speed controls. To select a micro controller, we first considered the control bandwidth. For reliable control, we determined that we need at least a 400 Hz loop frequency. The Arduino Uno can provide higher control frequencies and is easy to program and integrate with many different sensors. For those reasons we chose the Arduino Uno as the main process control board.

Receiver And Remote Controller: The Quad-Tilt-Wing UAV controls its orientation and altitude through a custom autonomous control system. The radio controller is used for sending reference commands to the control board and can take over if the control system fails or in non-ideal conditions (e.g. wind gusts).

Battery: The battery is arguably the most important (and heaviest) component of a UAV. We have selected an ENGPOW LiPo battery with a voltage of 11.1 V, a current capacity of 2200 mAh, and a continuous discharge rate of 20C. It weighs 170 g.

Sensors: Various sensors we use in the Quad-Tilt-Wing platform are detailed in the system architecture in Fig. 7. We use an inertial measurement unit (IMU) for attitude measurements and an ultrasonic sensor for altitude control. Additionally, current sensors and GPS are used to quantify the performance of the platform, which will be explained in more detailed in the following section.

2.5 System Architecture

The overall system architecture of the Quad-Tilt-Wing UAV is shown in Fig. 7. The system uses 4 control inputs (rotor speeds) for leveling and a 6-axis IMU sensor for sensory feedback . A Kalman filter reads the signal from the IMU and computes Euler angles and angle rates. We implemented a PID control system for leveling the Quad-Tilt-Wing UAV [23–25]. An ultrasonic sensor is used for altitude control of the Quad-Tilt-Wing UAV using a separate PID controller. Additionally, we use an XBee wireless module to communicate between the base station and the Quad-Tilt-Wing robot in a bidirectional fashion. We use two microcontrollers on board the Quad-Tilt-Wing. An Arduino Uno is used as the main control board [26], which is responsible for the main control loop at a frequency above 400 Hz. The second microcontroller (Arduino Fio) is used to collect flight data, such as continuously tracking the location of the Quad-Tilt-Wing UAV using the GPS sensor and measuring the battery voltage and current values. The Arduino Fio collects data during flight, and logs flight data them on a micro SD card. Thus, we can analyze and visualize the data after each experiment. The tilt mechanism is also controlled by the user from the base station through the XBee. The host XBee is connected to a PC and communicates with the local XBee connected to the microcontroller of the Quad-Tilt-Wing UAV. When the user sends a desired tilt angle from the base station, the microcontroller computes the input angle for the four-bar mechanism based on calibration data and rotates each tilt servo motor accordingly.

3 Experimental Results

In this section we describe our results from the wind tunnel experiments and all flight tests. Wind tunnel tests were conducted to investigate the changes in lift and drag forces for different tilt angles of the wing. In flight experiments, we tested

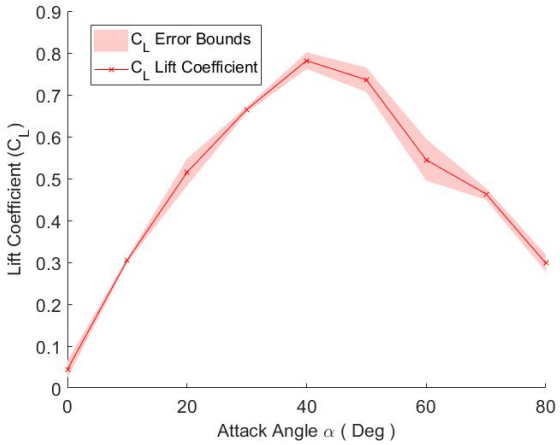

FIGURE 9. The Coefficient of Lift On Each Wing

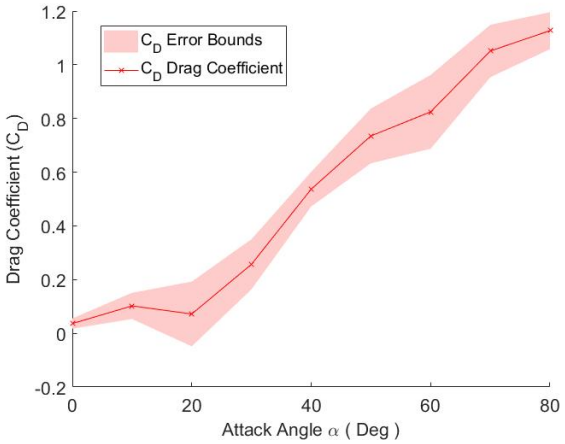

FIGURE 10. The Coefficient Of Drag On Each Wing

the full transition concept (vertical takeoff, horizontal flight, and vertical landing) of the Quad-Tilt-Wing UAV configuration and show flight performance during horizontal flight. Flight experiments were performed outdoors under calm wind speeds, video images were recorded for demonstration, and flight data was analyzed from the on-board measurements.

3.1 Wind Tunnel Testing

Wind tunnels are used to show how an object in flight behaves under reproducible conditions [27–29]. In this study, wind tunnel tests of the Quad-Tilt-Wing platform (shown in Fig. 8) have been carried out in the WPI Aerospace Engineering laboratories. Wing prototypes were mounted onto a custom-made three-component strain-gauge balance, which provides values for normal and axial force. The maximum load range is 111.2 N for the normal force and 44.4 N for the axial force. In this experiment, we used normal and axial force measurements to characterize the lift and drag coefficients of the wing. The wing model was installed in the wind tunnel test section and tested at various angles of attack α: 0°, 10°, 20°, 30°, 40°, 50°, 60°, 70°, and 80°) degrees. The wind speeds were specified between 20 m/s and 40 m/s. In a real flight test, the Quad-Tilt-Wing maximum air speed is 17m/s. Because the wind tunnel has low accuracy of measuring normal and axial force with low air speed, that is the reason we selected a higher airspeed during the wind tunnel experiment. However, once we compute the coefficients of lift and drag, we can recalculate lift and drag with real flight airspeeds at different tilt angles. The wind tunnel data was collected at all angle of attack values with different wind speeds, and analyzed for mean and standard deviation values to ensure accurate results.

Lift and drag data was then used to calculate the lift and drag coefficients as shown in Fig. 9 and 10 for angle of attack values between 0 and 80 degrees. Wind tunnel tests verify that the wings of the proposed platform generate a useful lift force when the angle of attack is close to 45 degrees and generate minimum lift forces at 0 or 90 degrees. This is in line with our expectations from the symmetric (flat-plate) shape of the wings. Similarly, the drag coefficient increases as the attack angle is increased, which leads to faster horizontal speeds for smaller tilt angles down to a minimum tilt angle of 25 degrees, below which the platform cannot generate enough lift force to keep afloat.

3.2 Flight Control System and Tuning Parameters

As described in Section 2, we use a classical (and effective) PID control system for attitude and altitude control of the Quad-Tilt-Wing UAV. The advantage of the PID controller is its feasibility and ease of implementation [25, 30]. The PID controller has to balance all three gains, which impact the whole system and errors such as settling time, overshoots, or oscillations may compromise the transient response. The PID gains can be tuned based on the system tracking errors. To adjust controller gains, we designed and built a parameter tuning stand. In this system, we used three potentiometers to manually adjust each gain (proportional, integral, and derivative) in real time. The the current parameter values were displayed on an LCD monitor. This tuning system helped us find a combination of gains by observing the resulting performance in real time and in a safe and controlled environment. In the design of the real-time parameter tuning stand, a central spherical joint was connected to a base platform and the Quad-Tilt-Wing UAV was allowed to operate in a spherical workspace constrained by the tuning system, allowing all three rotational degrees of freedom.

3.3 Full Flight Test

In the full flight test, the Quad-Tilt-Wing UAV takes off vertically, transitions to horizontal flight, and returns back to a stable hover before landing vertically. Thus, the tests consisted of three phases in sequence. The first is the vertical take-off quadcopter

TABLE 2. Tilt Angle and Speed

Tilt Angle (Degree)	Velocity (m/s)
80	3.595
70	6.198
60	7.66
40	9.392
30	12.86
25	17.26

phase (i.e. tilt angle 90°) where the UAV reaches a predefined height 1m. The second is the horizontal flight phase, in which the feedback control system for leveling and hovering is the same as in the quadcopter phase, except for a different tilt angle of the wing and rotors. Interestingly, the same control system can control the pitch, roll, and yaw of the Quad-Tilt-Wing platform using different control parameters tuned for each tilt angle during horizontal flight mode. The third phase is the vertical landing phase (i.e. tilt angle 90°), where the desired altitude was ground level and the thrust motors were turned off.

When conducting a full transition flight, we performed experiments where the tilt angles were fixed at 25°, 30°, 40°, 60°, 70° and 80° through the horizontal flight portion between takeoff and landing. When the tilt angle was above 80°, the Quad-Tilt-Wing worked well using the vertical hovering parameters. But for tilt angles less than 80°, we observed that the original parameters lead to oscillations in altitude as the Quad-Tilt-Wing accelerated through the horizontal motion, which eventually converged to a constant height. With the tuned parameter values, we reduced these oscillations to achieve a smooth transition to horizontal flight. We analyzed the experimental flight video data for each tilt angle and measured the average linear speed over the horizontal phase, as shown in Table 2. As expected, the Quad-Tilt-Wing platform can achieve relatively high linear velocities for its size for lower tilt angles, and can smoothly approach a zero-velocity hover as the tilt angle is increased to vertical.

3.4 Flight Performance Test (Linear Motion)

The goals of the flight performance tests were to measure the total flight distance, flight time, and total energy spent for different tilt angles during pure horizontal flight. We used two different test scenarios to accurately measure performance: flying the Quad-Tilt-Wing platform in 1) a linear path, which is closer to the real horizontal flight, but cannot provide long-range data; 2) a circular path, which is continuously changing the flight direction of the platform in a large diameter, thus allowing data collection until the battery is depleted at the expense of a slightly different trajectory from pure horizontal flight.

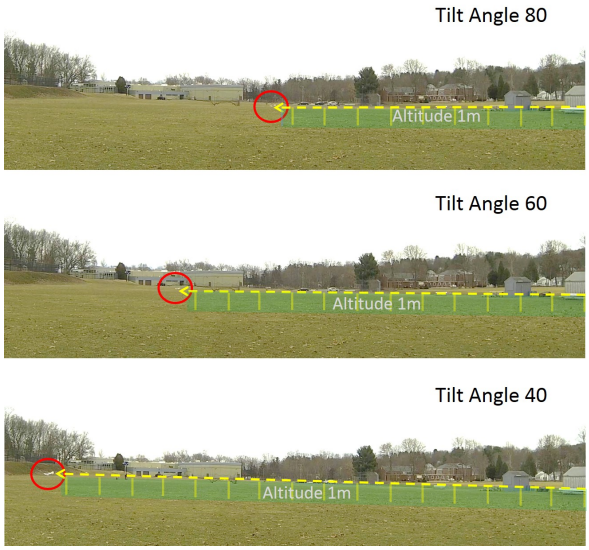

FIGURE 11. Full Flight Test (Linear Motion Performance Test)

Fig. 12 shows linear motion performance test results. In a linear trajectory, knowing that the flight distance is constant, we can compare flight time and energy expenditure at different tilt angles. In these experiments we tested tilt angle values of 40, 60 and 80 degrees (Fig.11) over a constant flight distance of 130 m. As we discussed in Section 2, the system logged electrical current and voltage data on a micro SD card during the flight. After each performance test, we analyzed the data using MATLAB.In Fig. 12, the top row displays the input electric power for each tilt angle. From electrical power information, we can calculate the total energy used over the flight distance. We can analyze the average energy expenditure over three bar graphs (d), (e), (f) representing total energy, energy per second and energy per meter. In addition, Fig. 13 displays the energy spent over the flight distance for each tilt angle (40°, 60°, 80°). These figures indicate that for lower tilt angles (high speed), energy expenditure was low. On the other hand, for larger tilt angles (low speed), the system used more energy to fly at the same altitude (1 m), suggesting that the wings contribute to lift and reduce energy needs for horizontal flight.

3.5 Flight Performance Test (Circular Motion)

In circular motion performance tests, we measured the total life time and average energy expenditure at three tilt-angle values of 50, 60 and 70 degrees. In this performance test, the Quad-Tilt-Wing UAV should fly until the battery is fully depleted. To achieve high-accuracy flight distance data we considered using circular flight trajectories with constant radii. In this case, GPS data would not be useful, because if we implemented path planning and used GPS measurements, we would accumulate errors in distance measurements. In this case, we used a simple method to achieve circular flight. A 9.5-m length of rope was attached

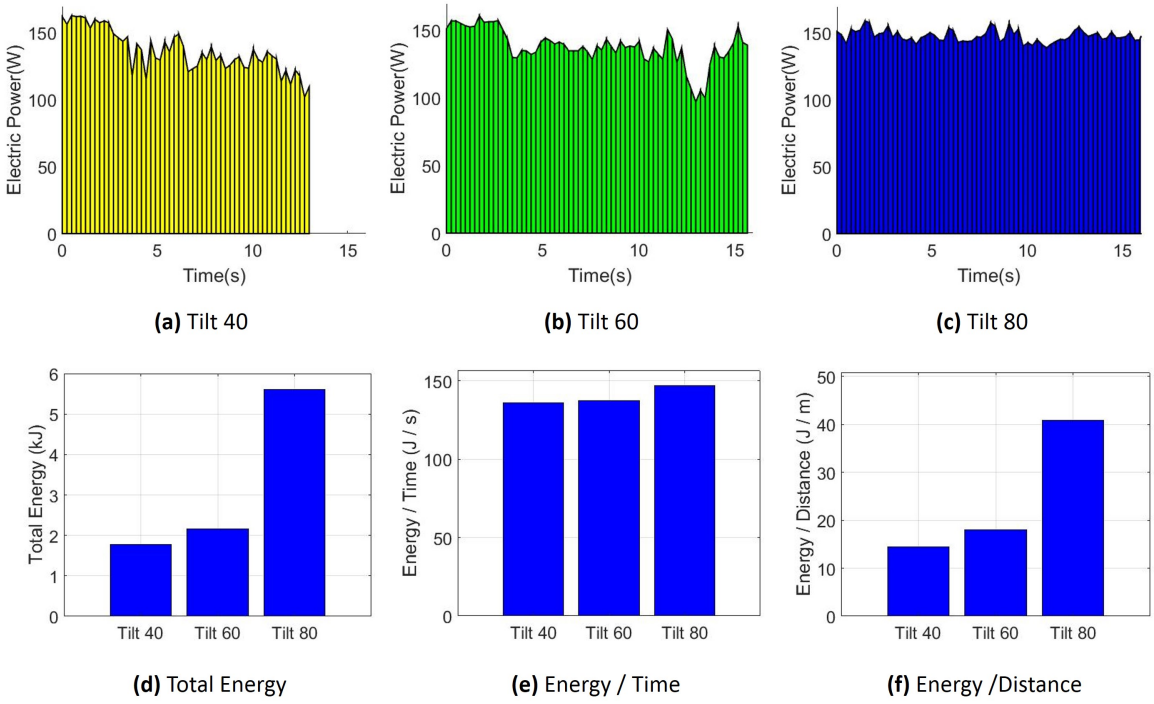

FIGURE 12. Linear Motion Performance Test Result (Tilt Angle 80, 60, 40). (a) Tilt Angle 40: Electric Power by Time. (b) Tilt Angle 60: Electric Power by Time. (c) Tilt Angle 80: Electric Power by Time. (d) Total Electric Energy. (e) Electric Energy by Time. (f) Electric Energy by Distance.

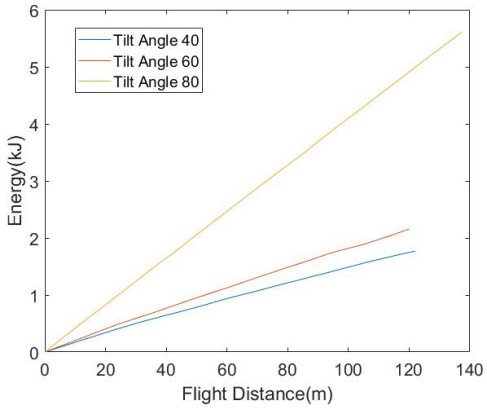

FIGURE 13. Spent Energy and Flight Distance

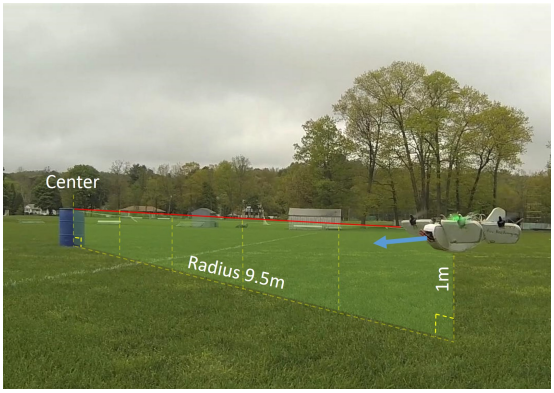

FIGURE 14. Circular Motion Performance Test

on one side to a fixed point (i.e. the center of the circle) and the other side was mounted to the Quad-Tilt-Wing UAV (Fig.14). As the platform tried to fly horizontally following a straight line, the rope pulled it aside into a circular motion. Because we knew the rope length we could calculate the flight distance by counting the number of cycles flown around the center in test video images.

In this performance test, we selected three different tilt angles based on initial experiments under these conditions. For tilt angles lower than approximately 50° the UAV achieves relatively high speeds but cannot maintain a purely circular flight motion due to external wind causing the Quad-Tilt-Wing platform to deviate from the circular path at constant altitude. Interestingly, for tilt angles larger than approximately 70 degrees, the UAV was not able to achieve a large enough linear speed to stay aloft. We believe the effect of the rope pulling the Quad-Tilt-Wing inside the circle has a detrimental effect when using the same control parameters as linear horizontal flight. Thus we settled on 50, 60, and 70 degree tilt angles. The circular motion performance test

TABLE 3. Circular Motion Performance Test Result

Measurements	Tilt 50	Tilt 60	Tilt 70
Number of revolutions:	67	64	44
Total flight time (s):	587.51	677.18	660.275
Total flight distance (m):	3999.2	3820	2641
Constant speed (m/s):	6.807	5.64	4

results are displayed in Table 3. As before, Fig. 15 represent the energy spent over flight distance using the three tilt angles. Between the two performance tests (linear and circular), we can compare the common experimental data for 60-degree tilt angle. For this tilt angle, the platform clearly spent more energy during circular motion than linear motion. We believe that in circular motion, the rope pulls the UAV in and causes a reduction in flight speed. Overall, the performance test results match what we expected. During horizontal flight, the wings generate lift and the platform effectively spends lower energy compared to vertical flight. Finally, our results show that the proposed Quad-Tilt-Wing design can achieve long duration flight with low energy consumption compared to conventional Multi-Rotor UAVs.

4 Conclusion and Future Work

In this paper, we proposed the mechanical design and autonomous attitude control system of a flying robot platform that combines the advantages of fixed-wing and rotary-wing UAVs. In our design, using rotor thrust as a source of lift in vertical flight, operating rotors as the forward propulsion sources, and wings as the lift sources in horizontal flight. Unlike current and previous twin-engine tilt wing vehicles and Quad-Tilt-Wing rotor vehicles, our Quad-Tilt-Wing platform does not require additional flaperon, elevator, or rudder control surfaces, which simplifies the control and has advantages over existing systems in payload carrying performance and energy efficiency. We described the mechanical design, prototyping principles, force analysis of flying robot platform, the attitude and altitude control system, the experimental results of wind tunnel test and full-conversion flight. Experimental flight test results demonstrate that the Quad-Tilt-Wing flying robot can successfully achieve full conversion flight with vertical takeoff, high speed cruising, and vertical landing, as well as super-short takeoff. Additionally, performance test results show that during horizontal flight, wings generate lift and reduce energy needs compared to vertical flight. In future work, we are considering the modeling flying platform and use path planning techniques to achieve highly maneuverable robotic flight functionality of the proposed platform. We will further explore those research directions in the future.

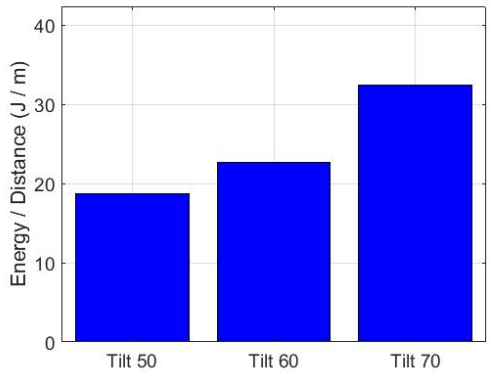

FIGURE 15. Circular Motion Performance Test Result

ACKNOWLEDGMENT

Wind tunnel tests were conducted with assistance from WPI Aerospace Engineering Department. The authors would like to gratefully acknowledge Prof. David J. Olinger's help with the experiments.

REFERENCES

[1] Jantawong, J., and Deelertpaiboon, C., 2018. "Automatic landing control based on gps for fixed-wing aircraft". In 2018 15th International Conference on Electrical Engineering/Electronics, Computer, Telecommunications and Information Technology (ECTI-CON), IEEE, pp. 313–316.

[2] Kumar, V., and Michael, N., 2017. "Opportunities and challenges with autonomous micro aerial vehicles". In *Robotics Research*. Springer, pp. 41–58.

[3] Nonami, K., Kendoul, F., Suzuki, S., Wang, W., and Nakazawa, D. Autonomous flying robots-unmanned aerial vehicles and micro aerial vehicles (2010).

[4] Boon, M., Drijfhout, A., and Tesfamichael, S., 2017. "Comparison of a fixed-wing and multi-rotor uav for environmental mapping applications: a case study". *The International Archives of Photogrammetry, Remote Sensing and Spatial Information Sciences,* ***42***, p. 47.

[5] Shaqura, M., and Shamma, J. S., 2018. "An iterative learning approach for motion control and performance enhancement of quadcopter uavs". In 2018 18th International Conference on Control, Automation and Systems (ICCAS), IEEE, pp. 285–290.

[6] De Lellis Costa de Oliveira, M., 2011. Modeling, identification and control of a quadrotor aircraft.

[7] Mustapa, Z., Saat, S., Husin, S., and Abas, N., 2014. "Altitude controller design for multi-copter uav". In Computer, Communications, and Control Technology (I4CT), 2014 International Conference on, IEEE, pp. 382–387.

[8] Takeuchi, R., Watanabe, K., and Nagai, I., 2017. "Devel-

opment and control of tilt-wings for a tilt-type quadrotor". In Mechatronics and Automation (ICMA), 2017 IEEE International Conference on, IEEE, pp. 501–506.

[9] Kang, Y.-S., Park, B.-j., Cho, A., Yoo, C.-s., and Choi, S.-w., 2013. "Envelop expansion flight test of flight control systems for tr-60 tilt-rotor uav". In 2013 13th International Conference on Control, Automation and Systems (ICCAS 2013), IEEE, pp. 1866–1871.

[10] Snyder, D., 2000. "The quad tiltrotor: its beginning and evolution". In Proceedings of the 56th Annual Forum, American Helicopter Society, Virginia Beach, Virginia.

[11] Lee, J.-H., Min, B.-M., and Kim, E.-T., 2007. "Autopilot design of tilt-rotor uav using particle swarm optimization method". In Control, Automation and Systems, 2007. ICCAS'07. International Conference on, IEEE, pp. 1629–1633.

[12] Helicopter, B., 2005. Eagle eye pocket guide.

[13] Naldi, R., Gentili, L., Marconi, L., and Sala, A., 2010. "Design and experimental validation of a nonlinear control law for a ducted-fan miniature aerial vehicle". *Control Engineering Practice,* ***18***(7), pp. 747–760.

[14] Sanchez, A., Escareno, J., Garcia, O., Lozano, R., et al., 2008. "Autonomous hovering of a noncyclic tiltrotor uav: Modeling, control and implementation". In Proc. of the 17th IFAC Wold Congress, Citeseer, pp. 803–808.

[15] Tran, A. T., Sakamoto, N., Sato, M., and Muraoka, K., 2017. "Control augmentation system design for quad-tilt-wing unmanned aerial vehicle via robust output regulation method". *IEEE Transactions on Aerospace and Electronic Systems,* ***53***(1), pp. 357–369.

[16] Suzuki, S., Zhijia, R., Horita, Y., Nonami, K., Kimura, G., Bando, T., Hirabayashi, D., Furuya, M., and Yasuda, K., 2010. "Attitude control of quad rotors qtw-uav with tilt wing mechanism". *Journal of System Design and Dynamics,* ***4***(3), pp. 416–428.

[17] Hochstenbach, M., Notteboom, C., Theys, B., and De Schutter, J., 2015. "Design and control of an unmanned aerial vehicle for autonomous parcel delivery with transition from vertical take-off to forward flight–vertikul, a quadcopter tailsitter". *International Journal of Micro Air Vehicles,* ***7***(4), pp. 395–405.

[18] Muraoka, K., Okada, N., and Kubo, D., 2009. "Quad tilt wing vtol uav: Aerodynamic characteristics and prototype flight". In AIAA Infotech@ Aerospace Conference and AIAA Unmanned... Unlimited Conference, p. 1834.

[19] Theys, B., Dimitriadis, G., Andrianne, T., Hendrick, P., and De Schutter, J., 2014. "Wind tunnel testing of a vtol mav propeller in tilted operating mode". In 2014 International conference on unmanned aircraft systems (ICUAS), IEEE, pp. 1064–1072.

[20] Alkamachi, A., and Erçelebi, E., 2017. "Modelling and control of h-shaped racing quadcopter with tilting propellers". *Facta Universitatis, Series: Mechanical Engineering,* ***15***, 08, pp. 201–215.

[21] Zhang, L., Wu, J., Liu, S., Wang, C., and Li, A., 2017. "Adaptive backstepping sliding mode controller design based on "h" type quadrotor". In Control Conference (CCC), 2017 36th Chinese, IEEE, pp. 3824–3828.

[22] Chamorro, W., Herrera, M., Camacho, O., Gómez, A., and Charro, F., 2017. "Design and robustness analysis of a sliding mode control for a quadrotor". In 2017 International Conference on Information Systems and Computer Science (INCISCOS), IEEE, pp. 60–65.

[23] Bao, N., Ran, X., Wu, Z., Xue, Y., and Wang, K., 2017. "Research on attitude controller of quadcopter based on cascade pid control algorithm". In Technology, Networking, Electronic and Automation Control Conference (ITNEC), 2017 IEEE 2nd Information, IEEE, pp. 1493–1497.

[24] Paiva, E., Soto, J., Salinas, J., and Ipanaqué, W., 2016. "Modeling, simulation and implementation of a modified pid controller for stabilizing a quadcopter". In Automatica (ICA-ACCA), IEEE International Conference on, IEEE, pp. 1–6.

[25] Sa, R. C., De Araujo, A. L. C., Varela, A. T., and Barreto, G. d. A., 2013. "Construction and pid control for stability of an unmanned aerial vehicle of the type quadrotor". In Robotics Symposium and Competition (LARS/LARC), 2013 Latin American, IEEE, pp. 95–99.

[26] Khavnekar, A., Gondalia, J., and Shah, D., 2017. "Low-cost arduino based architecture for simulation and control of quadrotors". In Inventive Systems and Control (ICISC), 2017 International Conference on, IEEE, pp. 1–6.

[27] Pandya, Y., Sreevanshu, Y., Sharma, A., Jain, K., Jena, S., Pawar, A. A., Ranjan, K. S., and Saha, S., 2017. "Aerodynamic characterization of a model aircraft using wind-tunnel testing and numerical simulations". In Recent Advances in Aerospace Engineering (ICRAAE), 2017 First International Conference on, IEEE, pp. 1–6.

[28] Fey, U., Egami, Y., and Klein, C., 2007. "Temperature-sensitive paint application in cryogenic wind tunnels: Transition detection at high reynolds numbers and influence of the technique on measured aerodynamic coefficients". In Instrumentation in Aerospace Simulation Facilities, 2007. ICIASF 2007. 22nd International Congress on, IEEE, pp. 1–17.

[29] Schauerhamer, D. G., Zarchi, K. A., Kleb, W. L., and Edquist, K. T., 2013. "Supersonic retropropulsion cfd validation with ames unitary plan wind tunnel test data". In Aerospace Conference, 2013 IEEE, IEEE, pp. 1–14.

[30] Sudha, G., and Deepa, S., 2016. "Optimization for pid control parameters on pitch control of aircraft dynamics based on tuning methods". *Applied Mathematics & Information Sciences,* ***10***(1), p. 343.